LAWRENCE
LIVERMORE
NATIONAL
LABORATORY

LLNL-JRNL-823585

Optimizing Power Systems Restoration with Damaged Communications

A. E. Musselman, I. A. Aravena Solis

June 16, 2021

Energy Systems

Energy Systems manuscript No.
(will be inserted by the editor)

Optimizing Power System Restoration with Damaged Communications

Amelia Musselman · **Ignacio Aravena**

Received: date / Accepted: date

Abstract Utility procedures for power system blackstart and restoration typically assume that energization decisions can be reliably communicated across the grid. In reality, the communications and control network would likely also be affected in power outages, such as those caused by extreme weather events or cyber-attacks. This paper studies the effect of damage to the power system communications and control infrastructure on restoration operations following a blackout. We model the communications infrastructure as a graph, overlaying the power grid, and imposing the requirement that every energized element in the power grid be observable from a control center. We expand on a specialized branch-and-bound algorithm from the literature to optimize the restoration process and devise an initialization heuristic and a rounding heuristic to improve solution speed. We perform numerical experiments on synthetic systems for Illinois and Texas with outages based on a solar flare or hurricane. We compare the results of our specialized branch-and-bound algorithm to the results from (i) the initialization heuristic alone, (ii) a variation of this heuristic that we use as a baseline, and (iii) the restoration optimization for the power system without communications constraints. We find that damage to the communications infrastructure significantly increases the time required to re-energize the grid. Moreover, by simultaneously optimizing communications repairs and grid energization decisions, we are able to re-energize the grid significantly faster than if communications repairs and energization decisions were made independently or with partial coordination, motivating improvements to current industry practice.

Amelia Musselman
Lawrence Livermore National Laboratory
Livermore, CA 94551 USA
E-mail: musselman5@llnl.gov

Ignacio Aravena
Lawrence Livermore National Laboratory
Livermore, CA 94551 USA
E-mail: aravenasolis1@llnl.gov

Keywords Communications network · power system control · power system restoration · resilience

1 Introduction

An essential aspect of power system resilience is the ability to quickly recover from an outage, whether it be from an extreme weather event, human error, or malicious attack. The ability to observe and control the network that is being restored is critical for effective power system restoration [35]. However, extreme weather events causing power system failures would likely affect the communications network controlling the grid as well. Inadequacy of communications and control systems has aggravated the impact of electrical disturbances in the past [25, 38]. Furthermore, in the case of a cyber-attack on the power grid, an attacker might decide to simultaneously attack the power system and the network controlling it in order to amplify damage and delay service restoration.

In this paper, we analyze the impact of failed communications systems on power system restoration following an electrical disturbance. We jointly optimize power system re-energization sequences and the repair of the communications system controlling the power grid. We develop the first model, that we are aware of, to jointly optimize power and communications system restoration decisions. To solve this model, we extend a specialized branch-and-bound algorithm previously developed and propose novel initialization and rounding heuristics to enhance the solution speed of this algorithm.

The paper is organized as follows. In the remainder of the present section we review relevant studies from the literature and give an overview of communications infrastructure for power systems. In Section 2 we formulate the optimal power system restoration problem with communications constraints. In Section 3 we describe our solution method and present initialization and rounding heuristics to improve solution speed. In Section 4 we describe the three case studies that were used to test our method and present experimental results. Section 5 summarizes our findings and conclusions. Nomenclature and the complete problem formulation are presented in Appendices A and B, respectively.

1.1 Literature Review

The control systems used to manage power systems were not originally designed to be connected to the internet and have become vulnerable to cyber-attacks [20, 30]. A number of researchers have assessed vulnerabilities in power system control networks. Ten et al. [34] develop a simulation-based approach to measuring vulnerabilities in Supervisory Control and Data Acquisition (SCADA) systems. Teixeira et al. [33] analyze ways in which an attacker could subvert bad data detection routines for state estimation in grid control systems. Sridhar et al. [29] present cyber-physical security requirements for power systems and give recommendations for research directions. Lai et al. [22] present an attacker-defender model to optimize grid hardening strategies against a joint attack on the transmission system and communications

network controlling it. Hong and Hoffman [19] characterize and propose mitigation actions against data injection attacks in outage management systems. Chikuni and Dondo [11] assess vulnerabilities of SCADA systems to cyber-attacks and give some recommendations for improving security. Dán and Sandberg [13] develop a security metric and an algorithm to determine the placement of encryption hardware to minimize state estimator vulnerability to attacks.

Even in the absence of a targeted attack, damaged communications systems can amplify the impact of an electrical disturbance. Simulations of communication failures in power systems show that increased communication failures can increase load shedding and cascading failures [25,28]. Motivated by this observation, Xie et al. [38] and Zhang and Vittal [39] propose redundant system architectures to increase communications resilience in power systems.

Existing research on optimal power system restoration (OPSR) largely neglects the potential impact of damaged communications. Zhong et al. [40] consider the effect of coupling networks on repair times but focus on analyzing the impact of coupling for various network structures when repairs are determined randomly. The most relevant works attempt to limit the impact of communication failures by adapting the optimal power flow problem [16] or managing node operations and power injections to ensure communication nodes remain operational [26]. To the best of our knowledge, no research has considered the problem of simultaneously optimizing power and communications system restoration after a disturbance impacting both systems. We address this problem, which we call OPSR-C.

Even without added complexity from communications, the OPSR problem corresponds to a mixed-integer, non-linear, non-convex program that is computationally hard to solve for networks of realistic size. A number of researchers have solved various linear programming approximations of the OPSR problem without communications [2, 3, 17, 31, 37]. However, their methods lack scalability. Aravena et al. [4] improve upon existing methods for OPSR by developing a specialized integer L-shaped method along with novel mixed-integer cuts and initialization and rounding heuristics, enabling the solution of larger instances of the OPSR problem than previously possible. However, [4] also assumes a fully functional communications system. In this paper, we extend the model and solution method from [4] to include the communications and control network governing the power system and simultaneously optimize the restoration of both systems. We analyze the impact of damaged communications on power system restoration (at the transmission level) and the benefit of simultaneously optimizing communications and power system repairs.

1.2 Communications in Power Systems

Electric grid operations largely rely on SCADA paired with energy management systems for monitoring and controlling the transmission network [11, 35]. SCADA systems collect data from intelligent electronic devices, most commonly via Ethernet connections, and use this data to monitor the power grid, either directly or via a user-interface for system operators [1, 15, 30]. SCADA systems typically operate under a master-slave model [15, 20]. Specifically, the control center (master) sends control

signals to the substations (slaves) in its control area. Components within a control center communicate via a local area network and the control center communicates with substations in its control area via a wide area network [30].

Other options for grid communications have also begun to be developed. Gungor and Lambert [18] survey some of these options, proposing Internet Based Virtual Private Networks as the base for network communications along with four options for connecting to rural substations lacking Internet access. All of these options (SCADA and alternatives) involve using a network structure to connect substations within a control area to their corresponding control center. This network structure is the basis for our model.

2 OPSR with Communications

We model the power and communications systems as interconnected graphs, which coincide at substations. In the power system graph, buses are nodes, power branches (lines and transformers) are edges, and substations are supernodes, each corresponding to a distinct subset of buses and the power branches interconnecting them. In the communications graph, substations and control centers are nodes, and communication channels are edges. While the power system graph is connected, the communications graph may not be connected and each connected component within it corresponds to a control area. Each control area has exactly one control center, which monitors and sends commands to power equipment at the substations within the control area using the communications graph, possibly relaying those communications through multiple substations.

Since attacking communications equipment at substations or control centers would cause more widespread damage than attacking a single communications channel, we only consider communications damage at substations and control centers. A communications channel is operational if and only if the communications equipment at both terminals (substations or control centers) of the channel is operational. If the communications equipment at a substation is damaged, the substation must remain de-energized for operational security. Control centers are always energized, possibly by backup generators or batteries, though the communications equipment at control centers may be damaged. A bus can only be energized if there is an operational communications path between the substation of that bus and the control center controlling that substation.

We solve a mixed integer program to optimize restoration sequences for the joint power-communications system from a given starting state in which power system equipment is either de-energized or energized, and communications equipment is either damaged or operational. Damaged communications equipment can be repaired by technicians, with each repair requiring one technician and taking a given number of time periods. Communication repairs are limited by the number of technicians available, and new energizations are limited by grid specifications. By optimizing restoration sequences for the two systems simultaneously, we seek to achieve shorter restoration times than if the two systems were considered separately.

2.1 Problem Formulation

Here we present our model for communications system restoration and how it relates to the power system restoration variables. Detailed nomenclature is presented in Appendix A. We include a compact description of the pure OPSR problem in Appendix B for completeness but refer the reader to [4] for further details regarding assumptions of the model and their implications. The OPSR problem aims to return the grid to normal operations as quickly as possible while maintaining feasibility in energization decisions and power flow. We use the same objective and constraints as in the OPSR problem and add the following constraints for communications restoration. The operational status of communication component a at time t is given by $w_{a,t}$ (valued 1 if operational, 0 if damaged), and $w^{\text{rep}}_{a,t}$ indicates if repair on the component begins at time t (valued 1 if repair starts, 0 otherwise). The energization status of bus n at time t is given by $u_{n,t}$.

We fix the status of communications equipment that is already operational at the start of the time horizon,

$$w_{a,t} = 1 \; \forall \; a \in C_0 \cup S_0, t \in T. \tag{1}$$

Communications equipment that is not operational at the start of the time horizon will become operational τ_a periods after it begins being repaired,

$$w_{a,t} - w_{a,t-1} = w^{\text{rep}}_{a,t-\tau_a} \; \forall \; a \in \{C \backslash C_0\} \cup \{S \backslash S_0\}, t \in \{1+\tau_a, \ldots, \overline{T}\}, \tag{2}$$

and its operational status must be 0 until enough time has passed for repairs to be completed,

$$w_{a,t} = 0 \; \forall \; a \in \{C \backslash C_0\} \cup \{S \backslash S_0\}, t \in \{1, \ldots, \tau_a\}. \tag{3}$$

Note that Constraints (1) – (3) imply that once communications equipment is operational, it will remain operational for the rest of the time horizon.

The number of substations and control centers simultaneously undergoing communications repairs is limited by the number of technicians available, K^{comm},

$$\sum_{a \in \{C \backslash C_0\} \cup \{S \backslash S_0\}} \; \sum_{t' = \max\{1, t-\tau_a+1\}}^{t} w^{\text{rep}}_{a,t'} \leq K^{\text{comm}} \; \forall \; t \in T. \tag{4}$$

Communications channels are operational if an only if the communications equipment at both terminals is operational,

$$w_{\ell,t} \leq w_{a,t} \; \forall \; \ell \in L^{\text{comm}}, a \in I^{\text{comm}}(\ell), t \in T, \tag{5}$$

$$w_{\ell,t} \geq \sum_{a \in I(\ell)} w_{a,t} - 1 \; \forall \; \ell \in L^{\text{comm}}, t \in T. \tag{6}$$

A bus, n, can only be energized if there is an operational communications path from its corresponding control center, $c(n)$, to the substation that bus is at, $s(n)$. To model this, we only allow a bus to be energized if the communications equipment at the control center for its substation is operational, the communications equipment

at its substation is operational, and there is an operational channel, ℓ, exiting every subset of substations containing that substation within the control area,

$$u_{n,t} \leq w_{c(n),t} \; \forall \; n \in N, t \in T, \tag{7}$$

$$u_{n,t} \leq w_{s(n),t} \; \forall \; n \in N, t \in T. \tag{8}$$

$$u_{n,t} \leq \sum_{\ell \in \delta(M)} w_{\ell,t} \; \forall n \in N, t \in T, M \subseteq S(c(n)) : s(n) \in M, \tag{9}$$

where $\delta(M)$ is the boundary of M, that is, the set of channels with one terminal in M and one terminal outside M, and $S(c(n))$ is the set of substations with the same control center as bus n. Constraints (7) – (9) give a stronger integer programming formulation than the single-commodity flow constraints used in [9], as shown in [27].

The energization status of buses must be feasible for the power system model,

$$u \in \mathscr{E}, \tag{10}$$

where $\mathscr{E}$ is the set of feasible energization decisions for buses in the OPSR problem, as defined in Equation (22) in Appendix B.

Finally, the indicator variables must be binary,

$$\begin{aligned} w_{a,t} &\in \{0,1\} \; \forall \; a \in C \cup S, t \in T, \\ w^{\text{rep}}_{a,t} &\in \{0,1\} \; \forall \; a \in C \cup S, t \in T. \end{aligned} \tag{11}$$

3 Solution Method

We adapt the decomposition algorithm developed in [4] for the OPSR problem to solve the OPSR-C problem $\{(1) - (11), (21)\}$.

Constraints (9) correspond to an exponential number of inequalities, which we handle via delayed constraint generation (i.e. mixed-integer optimizer *lazy* constraint callbacks). We start with the subset of Constraints (9) for which $M = \{s(n)\}$ for each $n \in N$. Each time a candidate solution satisfying (1) – (8) and (10) – (11) is found, we check for violated constraints by looking for connected components of operational elements in the communications graph that do not contain a control center but for which at least one substation has energized buses (thereby, violating Constraints (9)). If such a connected component exists, we add the constraints for the corresponding energized buses to Constraints (9), with M equal to the set of substations in the connected component, at the time period in which Constraints (9) were violated. We continue to generate constraints in this way until an acceptable (ε-optimal) solution is found.

In order to improve the runtime of the decomposition algorithm, we develop two supplementary heuristics, one to find an initial feasible solution and another to round fractional solutions found by branch-and-bound to integer solution candidates, described in the following sections. Additional notation used for these heuristics is defined in Appendix A.

3.1 Initialization Heuristic

We devise a greedy algorithm to quickly find a feasible initial solution to warm-start the branch-and-bound search with. A good initial solution can improve the branch-and-bound algorithm by providing a bound by which the algorithm can prune branches and a feasible solution to guide generic solver heuristics [24]. Our greedy algorithm seeks to construct a feasible communications repair and power restoration plan that would follow a pure power restoration plan as closely as possible, so as to minimize delays in energization caused by unreliable communications capabilities. The algorithm first builds a pure power restoration plan covering all periods, considering only stylized power system operational (power flow) feasibility requirements. The algorithm then incrementally builds a coordinated repair and restoration plan as follows: sequentially, for each period $t \in T$, with decisions from periods prior to t fixed, the algorithm decides (i) which damaged communications equipment to start repairing at period t, using estimated repair benefits constructed from the pure power restoration plan; and (ii) new energizations of power equipment at time t that honor the communications repair decisions.

The initialization heuristic is presented in Algorithm 1. We detail and justify the design of the algorithm below.

Algorithm 1: Initialization Heuristic

Input: Data for the OPSR-C problem, γ, and γ^{dist}.
For t=0, let $\tilde{\mathbf{u}}, \bar{\mathbf{u}}$, and $\mathbf{w}$ be 0 for initially inoperable elements and 1 otherwise.
Run *Relaxed Energization Init* for all periods to get $\tilde{\mathbf{u}}$.
for $t \in T$ **do**
  $\mathbf{w}_t \leftarrow \mathbf{w}_{t-1}$, $C_t^- \leftarrow C_{t-1}^-$, $S_t^- \leftarrow S_{t-1}^-$.
  Set $w_{a,t}^{\text{rep}} = 0 \; \forall \, a \in C \cup S$.
  if $t = 1$ **then**
    Set $w_{a,t} = 1, w_{a,t}^{\text{rep}} = 1 \; \forall \, a \in C_0^- \cup S_0^- \,|\, \tau_a = 0$.
  else
    Set $w_{a,t} = 1 \; \forall \, a \in C_0^- \cup S_0^- \,|\, w_{a,t-\tau_a}^{\text{rep}} = 1$.
  end
  for $c \in C$ **do**
    Calculate $z_{v,t}^{\text{en}} \; \forall \, v \in$ nodes of $\mathscr{G}_{ct}$.
    Find $MST(\mathscr{G}_{ct})$.
    Calculate $z_{v,t}^{\text{comm}}$.
  end
  Let $k = \sum_{a \in C_0^- \cup S_0^-} \sum_{t'=\max(t-\tau_a+1,1)}^{t-1} w_{a,t'}^{\text{rep}}$.
  while $k < K^{comm}$ **do**
    Choose $a \in C_t^- \cup S_t^- \,|\, z_{v_t(a),t}^{\text{comm}} = \max_{a' \in C_t^- \cup S_t^-} \{z_{v_t(a'),t}^{\text{comm}}\}$.
    Set $w_{a,t}^{\text{rep}} = 1$.
    If $a \in C_t^-$, $C_t^- \leftarrow C_t^- \backslash \{a\}$, else $S_t^- \leftarrow S_t^- \backslash \{a\}$.
    $k \leftarrow k + 1$
  end
  Do iteration t of *Energization Init* with Constraints (7) – (9) added and $\mathbf{w}$ and $\mathbf{w}^{\text{rep}}$ fixed to the values found up to time t. Set $\bar{\mathbf{u}}_t, \bar{\mathbf{u}}_t^{\text{CR}}$ to the resulting values.
end
return $\bar{\mathbf{u}}, \bar{\mathbf{u}}^{\text{CR}}, \mathbf{w}, \mathbf{w}^{\text{rep}}$

We refer to the initialization heuristic in [4], which does not consider communications constraints, as *Energization Init* and to the same algorithm but only with power grid connectivity requirements, i.e. that every energized bus must be connected to an energized generator, enforced instead of power flow feasibility, as *Relaxed Energization Init*.

Let $\tilde{\mathbf{u}}$ be the greedy pure power energization plan and $\bar{\mathbf{u}}$ be the greedy solution to the energization variables in the OPSR-C problem. For $t = 0$, we fix these variables to 0 for elements that are de-energized and 1 for elements that are already energized at the start of the time horizon. Similarly, the values of the communications variables, $\mathbf{w}$, at $t = 0$ are set according to the initial operational status of communications elements in the damage scenario. These variables are not defined for $t = 0$ in the model, but the initial state is required for the heuristic, which builds off the solution from the previous time period at each iteration.

We run *Relaxed Energization Init* for all time periods to get an initial energization solution, which we use to determine the value of communications repairs. We then loop through each time period, updating first the communications solution and then the energization solution for the current time period. For the communications system, since operational elements remain so for the rest of the time horizon, each iteration of the algorithm starts by setting the operational status of communications elements to the values from the previous period, in line 4 of Algorithm 1. Additionally, we initialize $w^{\text{rep}}_{a,t}$ to 0 at the current time period, in line 5. These values are later updated for elements that begin repair in the current period. We immediately repair any elements with $\tau_a = 0$, as shown in line 7, since they do not occupy repair technicians. We also update the operational status of any elements that have just completed repair in line 9.

Since our objective is to re-energize the grid as quickly as possible, the value of communications repairs depends on the energization benefit of the power system elements that those repairs would enable us to energize (once energization constraints are satisfied). To estimate this value, we first create a graph, $\mathscr{G}_t$, of the communications network at time t in which connected components of communications elements (substations or control centers) that are already operational at the start of period t are grouped into super-nodes, and damaged communications elements are each represented by a unique node. Edges are given by all communications channels that are not within a super-node. We determine the value of energizing buses at each node v of this graph according to the following equation,

$$z^{\text{en}}_{v,t} = \sum_{n \in N_t(v) | \bar{u}_{n,t-1}=0} \sum_{t' \in T} (1+\gamma)^{t-t'} \Bigg(\beta_n \tilde{u}_{n,t'} + \sum_{g \in G(n)} \beta_g \tilde{u}_{g,t'} + \sum_{\ell \in L(n) | \bar{u}_{\ell,t-1}=0} \frac{\beta_\ell}{2} \tilde{u}_{\ell,t'} \Bigg). \tag{12}$$

This function assesses the benefit over time of energizing buses and generators at the node and lines incident to the node. The benefit coefficients, β, represent the estimated benefit of energizing each element based on the OPSR objective function

(21).[1] The benefit is inflated by γ for elements that should have been energized in previous time periods but could not be, due to communications constraints, and discounted for elements that should be energized in future time periods. We divide the benefit of branches by 2 to distribute it between the two terminals.

For each control area, we find the minimum spanning tree of the corresponding sub-graph of $\mathscr{G}_t$, where edge weights are given by the average of the time to repair damaged terminals or 0 if the terminal is already operational at time t. The minimum spanning tree, defined in this way, reveals the path from the control center to each substation for which communications repairs could be completed most quickly. We use this information to determine the value of nodes that are along the shortest paths to other nodes from the control center.

The value for repairing damaged communications equipment at node v_1 of $\mathscr{G}_t$ is then given by,

$$z^{\text{comm}}_{v_1,t} = z^{\text{en}}_{v_1,t} + \sum_{v_2 \in \mathscr{V}_{ct}(v_1)} \frac{z^{\text{en}}_{v_2,t}}{(1+\gamma^{\text{dist}})^{\delta_{v_1 v_2 ct}}}, \tag{13}$$

and $z^{\text{comm}}_{v_1,t} = 0$ if the communications equipment at v_1 is already operational at time t. That is, the value of repairing damaged communications equipment is the value of energizing power system elements at the given node plus the discounted value of energizing power system elements at other nodes for which the path from the control center to the other node travels through the given node in the minimum spanning tree. Note that the substations and control centers within connected components are already operational because both terminals of communications channels must be operational for the channel to be operational, so super-nodes in the minimum spanning tree graph all have communications repair value of 0.

The steps for calculating the energization and communications values for each control area are shown in lines 11–15 of Algorithm 1. In line 16, we calculate the number of communications elements that are still under repair from previous time periods.[2] If this is less than the number of technicians, we rank the communications elements that still need to be repaired, $a \in C^-_t \cup S^-_t$, according to the communications value, $z^{\text{comm}}_{v_t(a),t}$, of the corresponding node, $v_t(a)$, of each element and start repair on as many of these elements as there are available technicians for, as shown in lines 17–22.

After fixing the communications solution found up to the current time period, we run a single iteration of the *Energization Init* algorithm with the communications constraints involving energization decisions added to find an energization solution for the current time period that is feasible for the fixed communications values (line 23). The algorithm then proceeds to the next time period. Upon completion, Algorithm 1 will produce a complete feasible solution for the OPSR-C problem, that is, a communications repair and power restoration plan.

[1] For branches and buses, β is exactly the value used in the OPSR objective function. For generators, we use the same coefficients but without the monotonically decreasing function, described in Appendix B, for simplicity.

[2] Although for $t = 1$, $w^{\text{rep}}_{a,t}$ will already be 1 by Step 16 if $\tau_a = 0$, elements with 0 repair time do not occupy repair resources and thus are not added to the total resources consumed.

3.2 Rounding Heuristic

In addition to the initialization heuristic, we also develop a rounding heuristic, presented in Algorithm 2, to assist the branch-and-bound algorithm in finding candidate integer solutions while exploring fractional nodes in the enumeration tree (see [24] for a description of the generic branch-and-bound algorithm). We cannot directly apply the rounding heuristic from [4] because communications elements take multiple time-periods to repair; thus, decisions cannot be decomposed by time without additional considerations. To address the inter-temporal nature of communication repairs, we keep track of elements that could not be repaired or energized in previous time periods and try to repair or energize them in later time periods, increasing the value of elements based on how many time periods it has been since they would have first been repaired or energized according to standard floating point rounding.

Algorithm 2: Rounding Heuristic

Input: A fractional candidate solution, $\tilde{\mathbf{u}}$, $\tilde{\mathbf{u}}^{\text{CR}}$, $\tilde{\mathbf{w}}^{\text{rep}}$, to and data for the OPSR-C problem. γ, N_0^-, L_0^-, G_0^-, G_0^{CR-}, C_0^-, and S_0^-.

Let $\tilde{u}^{\text{tot}}_{a,0} = 0 \; \forall \, a \in N_0^- \cup L_0^- \cup G_0^-$, $\tilde{u}^{CR,\text{tot}}_{g,0} = 0 \; \forall \, g \in G_0^{CR-}$, $\tilde{w}^{\text{rep,tot}}_{a,0} = 0 \; \forall \, a \in C_0^- \cup S_0^-$.

for $t \in T$ **do**

$\tilde{u}^{\text{tot}}_{a,t} = f(\tilde{u}^{\text{tot}}_{a,t-1}, \tilde{u}_{at}) \; \forall \, a \in N_{t-1}^- \cup L_{t-1}^- \cup G_{t-1}^-$,

$\tilde{u}^{CR,\text{tot}}_{g,t} = f(\tilde{u}^{CR,\text{tot}}_{a,t-1}, \tilde{u}^{\text{CR}}_{a,t}) \; \forall \, a \in G_{t-1}^{CR-}$,

$\tilde{w}^{\text{rep,tot}}_{a,t} = f(\tilde{w}^{\text{rep,tot}}_{a,t-1}, \tilde{w}^{\text{rep}}_{a,t}) \; \forall \, a \in C_{t-1}^- \cup S_{t-1}^-$.

Find the rounded values, $\bar{\mathbf{u}}_t$, $\bar{\mathbf{u}}_t^{\text{CR}}$, $\bar{\mathbf{w}}_t^{\text{rep}}$, by solving (15) at time t.

Update each of the sets as follows:

$$
\begin{aligned}
N_t^- &= N_{t-1}^- \setminus \{n \in N_{t-1}^- : \bar{u}_{n,t} = 1\}, \\
L_t^- &= L_{t-1}^- \setminus \{\ell \in L_{t-1}^- : \bar{u}_{\ell,t} = 1\}, \\
G_t^- &= G_{t-1}^- \setminus \{g \in G_{t-1}^- : \bar{u}_{g,t} = 1\}, \\
G_t^{CR-} &= G_{t-1}^{CR-} \setminus \{g \in G_{t-1}^{CR-} : \bar{u}^{\text{CR}}_{g,t} = 1\}, \\
C_t^- &= C_{t-1}^- \setminus \{c \in C_{t-1}^- : \bar{w}^{\text{rep}}_{ct} = 1\}, \\
S_t^- &= S_{t-1}^- \setminus \{s \in S_{t-1}^- : \bar{w}^{\text{rep}}_{st} = 1\}.
\end{aligned}
$$

end

return $\bar{\mathbf{u}}$, $\bar{\mathbf{u}}^{\text{CR}}$, $\bar{\mathbf{w}}^{\text{rep}}$

The rounding heuristic also takes a greedy approach, rounding one period at a time. In order to prioritize elements that should have been restored in previous time periods but could not be due to power system stability constraints or resource limitations, we assign a value to each component based on the relaxed solution with values that would be rounded up by standard rounding inflated by γ for each time period the corresponding component is not repaired or energized. We find these values, which

we call $\mathbf{x}^{\text{tot}}$, using the following function,

$$f(x^{\text{tot}}_{a,t-1}, x_{a,t}) = \begin{cases} (1+\gamma)x^{\text{tot}}_{a,t-1} + x_{a,t} & \text{if } x_{a,t} \geq 0.5, \\ (1+\gamma)x^{\text{tot}}_{a,t-1} & \text{otherwise.} \end{cases} \tag{14}$$

This function is applied iteratively in Algorithm 2 for each component that has not been energized (line 3) or begun cranking (line 4) or being repaired (line 5), depending on the component type, by the end of the previous time period. A_t^- represents the set of elements that remain de-energized or damaged by the end of time t, where A_0^- represents the starting state of the system. G_t^{CR-} represents the set of de-energized generators that have not begun cranking by time t, which for $t = 0$ is assumed to be all de-energized generators. The initial cumulative restoration value, $x^{\text{tot}}_{a,0}$, is set to 0 for all elements in line 1 of the algorithm.

The rounded values for time t are given by,

$$\begin{aligned} \bar{\mathbf{u}}_t, \bar{\mathbf{u}}_t^{\text{CR}}, \bar{\mathbf{w}}_t^{\text{rep}} = \text{argmax} & \sum_{a \in N_{t-1}^- \cup L_{t-1}^- \cup G_{t-1}^-} \tilde{u}^{\text{tot}}_{at} u_{at} + \sum_{a \in G_{t-1}^{CR-}} \tilde{u}^{CR,\text{tot}}_{at} u^{\text{CR}}_{at} \\ & + \sum_{a \in C_{t-1}^- \cup S_{t-1}^-} \tilde{w}^{\text{rep,tot}}_{at} w^{\text{rep}}_{at} - ||\tilde{\mathbf{u}}_t - \mathbf{u}_t||_1 \\ & - ||\tilde{\mathbf{u}}_t^{\text{CR}} - \mathbf{u}_t^{\text{CR}}||_1 - ||\tilde{\mathbf{w}}_t^{\text{rep}} - \mathbf{w}_t^{\text{rep}}||_1 \\ \text{s.t. Relaxed OPSR-C constraints up to time } & t, \\ u_{at} \geq \bar{u}_{at-1} \; \forall \; a \in N \cup L, & \\ \mathbf{u}_\tau = \bar{\mathbf{u}}_\tau \; \forall \; \tau \in \{1, \ldots, t-1\}, & \\ \mathbf{u}_\tau^{\text{CR}} = \bar{\mathbf{u}}_\tau^{\text{CR}} \; \forall \; \tau \in \{1, \ldots, t-1\}, & \\ \mathbf{w}_\tau^{\text{rep}} = \bar{\mathbf{w}}_\tau^{\text{rep}} \; \forall \; \tau \in \{1, \ldots, t-1\}, & \end{aligned} \tag{15}$$

where $\tilde{\mathbf{u}}_t$, $\tilde{\mathbf{u}}_t^{\text{CR}}$, and $\tilde{\mathbf{w}}_t^{\text{rep}}$ are the fractional solution values for time t. We consider $\mathbf{w}^{\text{rep}}$ instead of $\mathbf{w}$ for communications equipment because $\mathbf{w}$ is uniquely determined once the repair start times (indicated by $\mathbf{w}^{\text{rep}}$) have been chosen. $\tilde{u}^{\text{tot}}_{at}$, $\tilde{u}^{\text{CR,tot}}_{at}$, and $\tilde{w}^{\text{rep,tot}}_{at}$ represent the present value of energizing, cranking, and repairing, respectively, component a at time t. The objective function balances trying to restore elements that were not able to be restored in previous time periods with trying to match the fractional solution as closely as possible for the current time period. We enforce the OPSR-C constraints up to the current time period and fix the solution for all previous time periods, so only the solution for the current time period is found.

We assume buses and lines will remain energized once they have been energized. Problem (15) is solved to get a candidate integer solution[3] one period at a time in line 6 of Algorithm 2. The sets A_t^- are then updated to remove the newly energized elements or elements that just begun repair (line 7). G_t^{CR-} is also updated to remove generators that started cranking in the current period. The algorithm produces a candidate integer solution that accounts for discrepancies in previous periods' solutions

[3] Problem (15) may not produce a feasible solution to the original ORSR-C problem because we relax the OPSR-C constraints by only enforcing Constraints (20) for power system configurations that have already been identified. However, before updating the incumbent solution, the feasibility oracle checks the solution to (15) and adds cuts to prevent it from being explored again if it is infeasible.

while still only solving for one period at a time, which makes it efficient enough to be run at fractional branch-and-bound nodes, improving the global runtime of branch-and-bound.

4 Numerical Experiments

We test our model on synthetic case studies of Illinois and Texas representing damage from a solar flare or hurricane. We chose these two event types to represent the two types of damage that could occur to the combined power and communications system. A solar flare would damage the communications system and de-energize the power grid without actually damaging the power system elements. A hurricane, on the other hand, would damage both the communications system and the power system. Furthermore, a solar flare would damage the communications system through electromagnetic waves, which decrease in magnitude according to the square of the distance from the center of the disturbance. Damage from hurricanes is much more complex. We use historical data to approximate the hurricane's impact area, within which, for simplicity, we assume the damage probability decreases linearly from the hurricane center to a cutoff radius. The actual impact within the damage radius would depend on a number of factors including wind direction and terrain. Modeling these factors is outside of the scope of this work. Historical examples of the potential impact that these two types of events can have on the power grid are given in [35].

4.1 Synthetic Test Data

We use the transmission network (buses, branches, and substation data), demand, and bounds on generator power output from the synthetic test cases in [8]. We estimate other mechanical parameters of generators relevant to restoration – e.g. cranking time, cranking power, and inertia – based on public information for generators in the Chilean power grid [12][4]. We randomly assign blackstart capabilities to thermal generators under 50MW such that the fraction of these generators that are blackstart is similar to what is observed in real networks such as the Chilean grid and the PG&E grid [10].

To generate a synthetic communications and control network for each case study, we start from the power system data and partition the substations into control areas, fdedicating one control center to each control area. We choose the number of control areas such that there are at most 50 substations per control area and then partition the substations approximately evenly across these control areas while ensuring that each control area corresponds to a contiguous subnetwork of the power grid. We include a communications channel wherever there is a transmission line between two substations within the same control area. Within each control area, we randomly select substations to be adjacent to the control center such that at least 10% of the substations within each control area are adjacent to the control center. No communication

[4] The Chilean grid faces restoration and blackstart events continuously due to seismic nature of the country, hence, blackstart parameters of generators are measured and have been verified in real conditions.

channels between control areas are considered. The substation locations are included with the power system data [8]. We use the average location of substations adjacent to the control center as the control center location. The resulting Illinois test system has 200 buses, 179 lines, 3.54 GW generation capacity across 49 generators, 3 control centers, 111 substations, and 155 communications channels. The Texas test system has 2000 buses, 2345 lines, 100.09 GW generation capacity across 544 generators, 25 control centers, 1250 substations, and 1742 communications channels.

We consider three types of communications outages: damage from a solar flare with the impact centered on (*i*) Chicago, Illinois or (*ii*) Austin, Texas and (*iii*) damage from a hurricane similar to Hurricane Harvey in Texas. For the solar flare cases, we restrict communications damage to a 500 km radius disc. We assume that communications elements within this radius are damaged with a probability inversely proportional to the square of the distance to the center of the event. This probability takes the value of 1 at the center and decreases quadratically to a probability of 0.1 at the edge of the damage disc. Outside of the damage disc, all communications elements are operational (except for communications channels with one damaged terminal inside the disc and the other outside).

For the hurricane case, we use a center of damage and damage radius based on Hurricane Harvey. According to [23], Hurricane Harvey made landfall in Texas at a latitude of 28.0N and longitude of 97.0W, which we use as the damage center. For the damage radius, we calculate the distance between the maximum latitude and longitude and the minimum latitude and longitude in the "FilteredPeaks" spreadsheet found at [36] and halve this value to get a damage radius of 293.8 km. We assume a damage probability of 0.4 at the damage center, which decreases linearly to 0 at the damage radius.

The focus of the present study is on analyzing re-energization sequences and communication repairs with damaged communications components. Damaged power system components are removed from the system since the time to repair damaged power system components is longer than the length of the time horizon considered; thus we assume damaged power components will remain offline for the duration of the time horizon. Damaged power system components can take weeks to repair or replace, amplifying the importance of optimizing re-energization sequences to minimize load loss while waiting for these repairs to be made. In order to directly compare the impact of communications damage across all scenarios, we use the full synthetic test system as the starting state after damage has occurred (i.e. we assume that damaged power system elements have already been purged from the system data). Furthermore, for consistency in measuring the impact of communications damage on the power system, we assume a total power blackout in all cases.

Using these parameters, we generate 10 damage scenarios for each of the three outage types. Repair times for communications elements are generated using an exponential distribution with $\lambda = 1$ hour. We optimize restoration over a 12-hour time horizon, with 15-minute time increments for Illinois and 30-minute time increments for Texas (reducing resolution reduces the size of the mathematical program to solve).

We implement the OPSR-C model in Julia [5] using JuMP [14] and solve it with Gurobi. We run our specialized branch-and-bound algorithm, with the initialization and rounding heuristics included, with a wall clock limit of 24 hours or until a 1%

optimality gap is achieved, whichever comes first. We compare these results with the results of the initialization heuristic alone, as well as a modified initialization heuristic where the energization solution in step 1 of Algorithm 1 is replaced by $\tilde{\mathbf{u}} = 1$. We use the latter as our baseline because we believe it best represents what would be done in practice to restore communications, although current industry power restoration plans assume a fully functioning communications system [32]. This variation of the algorithm makes communications repair decisions by considering the energization benefit of substations (i.e. energization priorities) and the communications network structure, but without first optimizing the energization decisions for the current outage situation. We improve on this method in the initialization heuristic by solving the energization problem both before and after the communications solution is found. We also compare against an optimal plan for pure power restoration (i.e. the result of the OPSR model in [4]) to analyze the impact of communications constraints on power system restoration.

4.2 Results

Figure 1 shows the objective values across scenarios, ordered within each outage type from lowest to highest objective value found by the branch-and-bound algorithm. We only present results for one hurricane scenario in the plots because, as this outage type has a smaller impact on the communications system, there is only a small difference in objective values between the most and least damaging hurricane scenarios (3.4% difference in branch-and-bound objective value versus 12.6% for the Texas solar flare case).

For Illinois, the optimal objective value for the OPSR model is 24-41% higher than all of the OPSR-C scenarios, demonstrating the large impact of damaged communications on power system restoration. Across the Illinois solar flare scenarios, the objective values found by the branch-and-bound algorithm are between 15-59% better than the initialization heuristic and 17-429% better than the baseline. For Texas, the objective value for the best solution found for the OPSR model is 0.36-13% higher than the objectives found for the solar flare scenarios and 2.4-5.9% higher than those found for the hurricane scenarios. However, in none of the Texas damage scenarios or the OPSR model is the algorithm able to reach the target optimality gap within the 24-hour wallclock time limit. The optimality gap at 24 hours is 38% for the OPSR model, 30-48% for the solar flare scenarios, and 38-49% for the hurricane scenarios. Even with such high gaps for the Texas solar flare scenarios, the branch-and-bound algorithm improves on the initialization heuristic by 0.07-0.22% and improves on the baseline by 2.3-14% in all but one of the scenarios. In the remaining scenario, *Solar flare 2*, the solution obtained by the branch-and-bound algorithm is 1.1% worse than the baseline, which is possible because the baseline solution is not used to initialize the branch-and-bound algorithm. For the Texas hurricane scenarios, since there is not as much damage to the communications system, the initialization heuristic and the baseline solutions give the same objective values, and the branch-and-bound algorithm improves on both algorithms between 0.18-1.3%.

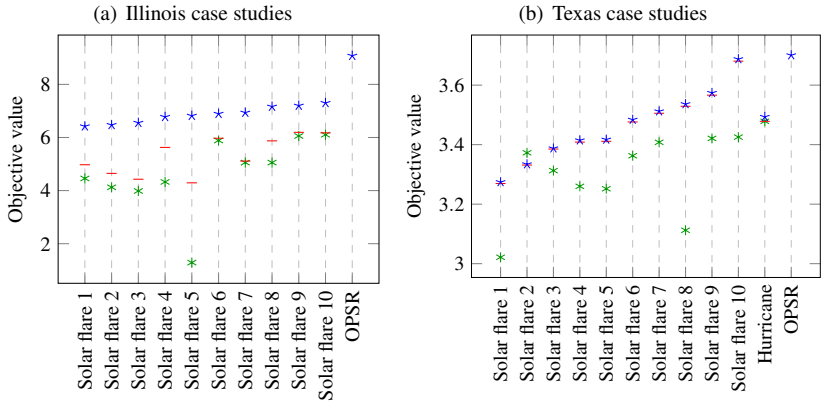

Fig. 1 Objective values found by each approach across damage scenarios. Blue stars mark the values attained by our specialized branch-and-bound algorithm, red horizontal lines mark the values attained by our initialization heuristic, and green asterisks mark the values attained by the modified heuristic which we use as a baseline. OPSR denotes the relaxed model without communications [4]. Only one hurricane scenario is plotted since the results are similar across scenarios.

Table 1 shows the minimum, maximum, and average difference between algorithms in the number of elements (or capacity in the case of generation) restored by the end of the time horizon for each of the three damage types. The branch-and-bound algorithm is compared to the initialization heuristic and to the baseline.

For Illinois, when comparing the branch-and-bound algorithm to the initialization heuristic, an average of 6.1% more buses, 9.6% more lines, 18.6% more generation capacity, 4.5% more substations, and 7.1% more communications channels are brought online by the end of the time horizon. The difference is even greater when comparing the branch-and-bound algorithm to the baseline, with 8.4% more buses, 9.3% more lines, 24.2% more generation capacity, 4.5% more substations, and 6.4% more communications channels brought online by the end of the time horizon, on average. The number of online control centers is the same for all algorithms, since there are only 3 total and all are able to be brought online by the end of the time horizon in all cases.

For Texas, the results are mixed. Across both outage types, more buses are brought online in the branch-and-bound solution by the end of the horizon than in both the initialization heuristic and the baseline in all but one solar flare scenario. However, at least as many, and sometimes more, control centers, substations, and communications channels are brought online by the heuristics as by the branch-and-bound algorithm. For lines and generation capacity, it varies.

In general, the heuristic and baseline tend to repair more communications elements early in the time horizon. However, doing so doesn't necessarily lead to more rapid energization overall. For Illinois, by the end of the time horizon, more communications elements have been repaired in the branch-and-bound algorithm than in the heuristics, even though in most cases the heuristics had restored more communications elements early in the time horizon. We are unable to make the same conclusion about Texas since the system is not fully energized by the end of the time horizon.

Table 1 Difference in elements restored by the end of the time horizon for the three damage types.

Metric	Damage type	Branch-and-bound to heuristic difference			Branch-and-bound to baseline difference		
		Min.	Avg.	Max.	Min.	Avg.	Max.
Number of buses	IL solar flare	-6	12.1	43	-1	16.7	41
	TX solar flare	-1	1.4	3	0	10.7	19
	TX hurricane	0	2.5	6	0	2.5	6
Number of lines	IL solar flare	-3	17.2	36	-2	16.6	33
	TX solar flare	0	0	0	-31	16.3	54
	TX hurricane	-1	-0.1	0	-1	-0.1	0
Generation capacity (MW)	IL solar flare	195	659	948	419	856	994
	TX solar flare	-2.3	171	597	-4308	-922	3112
	TX hurricane	0	388	1171	0	388	1171
Num. of control centers	IL solar flare	0	0	0	0	0	0
	TX solar flare	0	0	0	-1	-0.2	0
	TX hurricane	0	0	0	0	0	0
Number of substations	IL solar flare	1	5	10	1	5	12
	TX solar flare	-14	-9.7	-1	-44	-33	-13
	TX hurricane	-1	-0.1	0	-1	-0.1	0
Number of comm. channels	IL solar flare	5	11	24	0	9.9	21
	TX solar flare	-30	-18.7	-3	-89	-58.3	-27
	TX hurricane	-3	-0.3	0	-3	-0.3	0

Focusing on a specific scenario, Figure 2 shows the percent of elements (or percent of capacity, for generation) restored over the time horizon for Illinois solar flare scenario 5, the scenario for which the difference in objective value between the branch-and-bound algorithm and the two heuristics was the greatest. In this scenario, only one of the three control centers is damaged at the start of the time horizon. This control center is repaired first in the baseline algorithm and is repaired in the initialization heuristic one period before it is in the branch-and-bound algorithm. The baseline repairs substations communications more quickly than the branch-and-bound algorithm until hour 3.5 of the time horizon, at which point the branch-and-bound algorithm surpasses it. The initialization heuristic also exceeds or equals the branch-and-bound algorithm for a few of these initial periods, but after hour 3.5, follows a similar pattern to the baseline for substation repairs. A similar trend is observed for communications channels, which aren't repaired directly, but depend on substation and control center repairs. For buses, lines, and generation capacity, energization is zero across all three algorithms for the first 1.5 hours for buses and generators and 2 hours for lines. After this point, the branch-and-bound algorithm begins energizing elements and exceeds the initialization heuristic and baseline in elements energized, for the remainder of the time horizon. The initialization heuristic also exceeds the baseline once it begins energizing elements an hour later in the time horizon. It should be noted that the total load is about 42% of generation capacity, which is why

only around 50% of generation capacity is online by the end of the time horizon in the optimal solution.

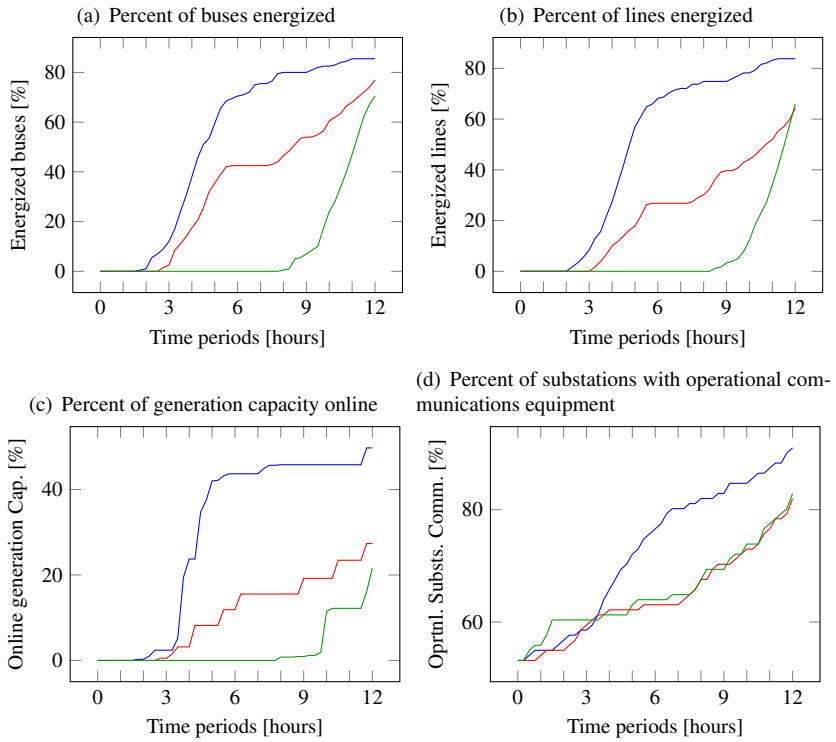

Fig. 2 Percent of elements restored over time in Illinois solar flare scenario 5. The branch-and-bound solution is shown in blue, the initialization heuristic in red, and the baseline in green.

Looking at a specific elements of this example, when the communications system is not considered at all, the power system solution starts by energizing buses at Substation 23, which has five generators connected to it, two of which two are blackstart generators. There is only one communications channel adjacent to Substation 23, and it is inoperable in the initial communications system for this scenario. The initialization heuristic builds a communications path from Control Center 1 to Substation 23, and simultaneously finishes cranking the two blackstart generators at this substation 2.75 hours into the time horizon. At the same time, an operational communications path from Control Center 2 to Substation 88 is completed, and the blackstart generator at this substation also finishes cranking. Substation 88 is also the second substation to be energized in the pure power solution. The energization sequence in the initialization heuristic follows the pure power solution the most closely of the the three algorithms, which makes sense since communications decisions are made in the initialization heuristic based on a greedy pure power solution. One distinction, however, is that the initialization heuristic energizes the system starting from all

three substations with blackstart generators, and the energized portion of the system isn't fully connected until 10.5 hours into the time horizon. In contrast, the OPSR solution (without communications) energizes the system starting from only two of the three substations with blackstart generators, connects the energized portion of the grid 1.5 hours into the time horizon, and continues expanding the energized system from this single component. The final substation with a blackstart generator to be energized in both cases is Substation 34, which is energized via the blackstart generator at hour 4.25 in the initialization heuristic, but connected to the already energized grid at hour 2 in the solution without communications. The initialization heuristic is the only of the three algorithms with communications to energize all three substations with blackstart generators.

The branch-and-bound and baseline solutions are very different from both the OPSR and initialization heuristic solutions, as well as from each other. The baseline repairs the control center and substations in such a way that more communications channels become operational early in the time horizon, but the combination of these channels doesn't create an operational communications path to any of the substations with blackstart generators. Furthermore, at hour 1.5, the baseline heuristic starts repairing communications equipment at three substations, two with over 3-hour repair times and the third with over a 2-hour repair time. Repairing these elements prevents any other elements from starting repair for the next 2 hours, by which point the branch-and-bound algorithm has surpassed the baseline in communications system repairs. 8 hours into the time horizon, the baseline heuristic finally completes an operational communications path to one of the blackstart generators, energizing first Substation 34. The baseline algorithm expands from this component to energize the power system until hour 9.25 at which point an operational communications path to Substation 88 is completed, and the blackstart generator at this substation, which finished cranking early on, can finally be connected to the power grid. The algorithm quickly connects the two energized components, but never completes a communications path to energize Substation 23, the third substation with a blackstart generator.

Rather than building an operational path to the first component to be energized in the OPSR solution, as the initialization heuristic does, or repairing communications elements to quickly connect as much of the grid as possible to the control centers, as the baseline does, the branch-and-bound algorithm focuses the repair resources on completing an operational path from Control Center 2 to Substation 88. It also repairs substations that complete communications paths starting from Substation 88, so the system can quickly be energized by expanding out from this substation. Substation 34 isn't energized until 7.5 hours into the time horizon, and even then it is energized by connecting to the already energized grid rather than using the blackstart capabilities to energize a new component. Substation 23, the third substation with blackstart generators, is not energized by the end of the time horizon in this solution.

Figure 3 shows the elements that have been restored by hour 5 of the time horizon, the first hour at which all transmission lines have been energized in the OPSR solution, for Illinois solar flare scenario 5. A map of the region of Illinois that the test system covers can be found at [7].

We see that, in this example, the branch-and-bound algorithm outperforms the other two algorithms by focusing all of its communications repair resources on com-

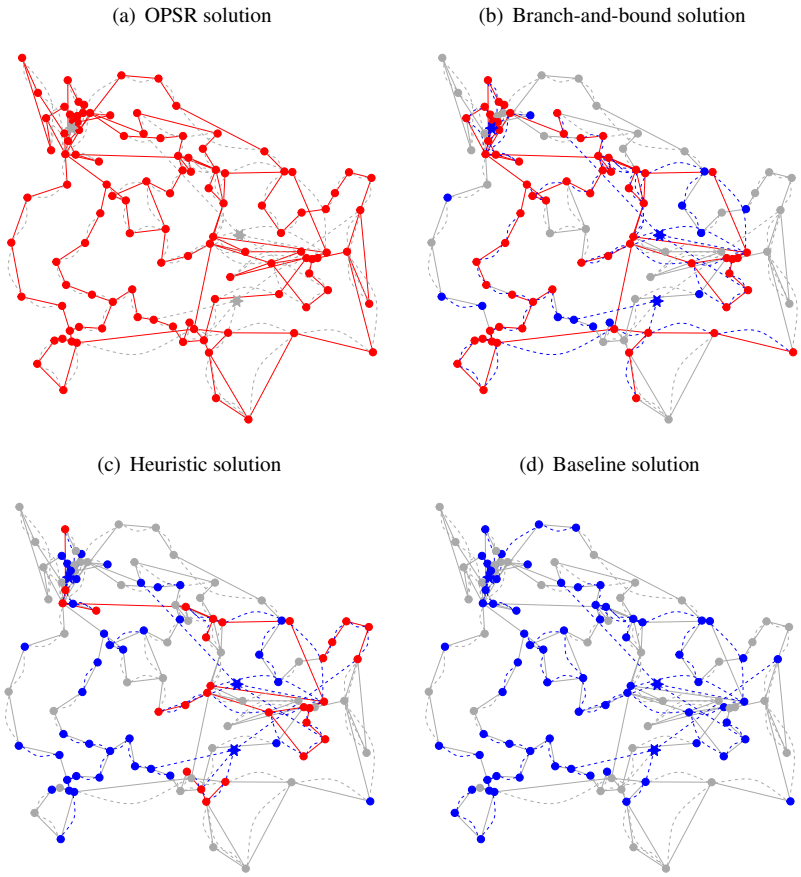

Fig. 3 Graph representing system status at hour 5 for Illinois solar flare scenario 5. Each node corresponds to a substation (circle) or control center (6-point star). Solid lines represent transmission lines; dashed lines represent communications channels. Substations that are not energized are colored blue if the communications equipment is operational. Operational communications channels and control centers are also colored blue. Energized transmission lines and substations are colored red. Offline/damaged elements are shown in gray.

pleting paths starting from only one of the three substations with blackstart generators. The heuristics were weakened by splitting repair resources across (at least two out of three of) these substations. When the power system is energized without communications constraints, blackstart generators can be energized at any time. However, when communications constraints are added, the wait time imposed by repairing communications elements may make a blackstart generator that was otherwise the most valuable for blackstarting the system less efficient. Thus, determining elements to energize or repair sequentially can lead to sub-optimal decisions. By co-optimizing communication repairs and energization decisions, we are able to capture the intricacies of how the communications system impacts the power system and find more realistic and better energization decisions.

5 Conclusions

In this work we develop a mixed-integer program to simultaneously optimize power system energization and communications repairs following an extreme event impacting both systems. We expand on a specialized branch-and-bound algorithm from the literature that solves the problem without communications [4]. Additionally, we (*i*) describe an effective constraint generation method to handle observability constraints between the communications and power networks and (*ii*) develop rounding and initialization heuristics to improve solution runtimes. We test our model and solution algorithm on synthetic test cases for Illinois and Texas with communications system damage representing the impact from a solar flare or hurricane. We compare the results of our algorithm to those found by the initialization heuristic alone and by a modified version of the initialization heuristic designed to approximate how decisions are currently made in practice. Additionally, we compare to the power system energization results when communications constraints are not included.

We find that including communications constraints in the energization model has a large impact on power system restoration. Without communications, all transmission lines in the Illinois test system can be energized by hour 5 of the time horizon when starting from a total blackout. With communications constraints, however, not all transmission lines are energized, even by the end of the 12-hour time horizon.

For the scenarios with communications damage, our algorithm always improves on the initialization heuristic and outperforms the baseline in all but one of the scenarios tested. For the Texas scenarios, the improvements from the initialization heuristic are small, but larger improvements are made compared to the baseline in all scenarios except one of the Texas solar flare scenarios. For the Illinois scenarios, large improvements are made compared to both the initialization heuristic and the baseline. Such large improvements in restoration performance might be possible for the Texas system as well, as the branch-and-bound algorithm's optimality gap was still over 30% at the 24-hour time limit, indicating that our restoration plans could be further improved significantly. The inability to close the optimality gap in the Texas scenarios is likely due to the large size of the system, which results in a larger mathematical program requiring larger times to solve relaxations and more extensive exploration of the branch-and-bound tree, making it harder to find feasible solutions and to strengthen upper bounds.

In future work, we would like to improve the scalability of our algorithm in order to better solve larger systems. One possible approach might be to explore characteristics of good solutions to improve our initialization heuristic. For example, by looking more closely at one of the Illinois scenarios, we found that it is better to repair communications along paths starting from a single substation with a blackstart generator than to repair communications in the neighborhoods of all of the blackstart generators. If a similar pattern was observed in other cases, the initialization heuristic could be modified to focus on one substation (or a few, for larger systems) with a blackstart generator, rather than splitting resources across all of them. Another unexplored avenue for improvement is the study of strengthening inequalities involving both the communications and power network, which would lead to better bounds and

better (closer to integer) candidate solutions being found by the branch-and-bound algorithm.

Acknowledgements This work performed under the auspices of the U.S. Department of Energy by Lawrence Livermore National Laboratory under Contract DE-AC52-07NA27344. The authors would like to thank Gurobi for providing licenses to the Gurobi Optimizer. We would also like to thank Brian Kelley for providing feedback on our communications model and the anonymous reviewers whose feedback helped to improve the quality of this paper.

This version of the article has been accepted for publication, after peer review but is not the Version of Record and does not reflect post-acceptance improvements or any corrections. The Version of Record is available online at: `http://dx.doi.org/10.1007/s12667-022-00553-0`. Use of this Accepted Version is subject to the publisher's Accepted Manuscript terms of use `https://www.springernature.com/gp/open-research/policies/acceptedmanuscript-terms`.

6 Declarations

Funding

This work performed under the auspices of the U.S. Department of Energy by Lawrence Livermore National Laboratory under Contract DE-AC52-07NA27344.

Conflict of Interest

The authors declare that they have no conflict of interest.

Availability of Data and Material

The data for the synthetic power systems was from Texas A&M's Electric Grid Test Case Repository documented in [8], with Texas data available at [6] and Illinois data available at [7]. Restoration and outage parameters are as described in Section 4. The specific random scenarios generated are not publicly available.

Code Availability

The code for this work is not publicly available.

References

1. Ali, I., Thomas, M.S.: Substation communication networks architecture. In: 2008 Joint International Conference on Power System Technology and IEEE Power India Conference (2008)
2. Arab, A., Khodaei, A., Khator, S.K., Han, Z.: Transmission network restoration considering AC power flow constraints. In: 2015 IEEE International Conference on Smart Grid Communications (SmartGridComm), pp. 816–821 (2015). DOI 10.1109/SmartGridComm.2015.7436402
3. Arab, A., Khodaei, A., Khator, S.K., Han, Z.: Electric power grid restoration considering disaster economics. IEEE Access **4**, 639–649 (2016). DOI 10.1109/ACCESS.2016.2523545
4. Aravena, I., Rajan, D., Patsakis, G., Oren, S.S., Rios, J.: A scalable mixed-integer decomposition approach for optimal power system restoration. Optimization Online pp. 1–8 (2019)

5. Bezanson, J., Edelman, A., Karpinski, S., Shah, V.B.: Julia: A fresh approach to numerical computing. SIAM review **59**(1), 65–98 (2017). URL https://doi.org/10.1137/141000671
6. Birchfield, A.B., Xu, T., Gegner, K.M., Shetye, K.S., Overbye, T.J.: Electric grid test case repository: ACTIVSg2000: 2000-bus synthetic grid on footprint of texas. Accessed July 22, 2021 at https://electricgrids.engr.tamu.edu/electric-grid-test-cases/activsg2000/
7. Birchfield, A.B., Xu, T., Gegner, K.M., Shetye, K.S., Overbye, T.J.: Electric grid test case repository: Illinois 200-bus system: ACTIVSg200. Accessed April 9, 2021 at https://electricgrids.engr.tamu.edu/electric-grid-test-cases/activsg200/
8. Birchfield, A.B., Xu, T., Gegner, K.M., Shetye, K.S., Overbye, T.J.: Grid structural characteristics as validation criteria for synthetic networks. IEEE Transactions on Power Systems **32**(4), 3258–3265 (2017)
9. Byeon, G., Hentenryck, P.V., Bent, R., Nagarajan, H.: Communication-constrained expansion planning for resilient distribution systems. INFORMS Journal on Computing pp. 1–18 (2020)
10. California ISO: Black start and system restoration phase 2. Accessed April 15, 2021 at http://www.caiso.com/informed/Pages/StakeholderProcesses/CompletedClosedStakeholderInitiatives/BlackStart_SystemRestorationPhase2.aspx
11. Chikuni, E., Dondo, M.: Investigating the security of electrical power systems scada. In: AFRICON. Windhoek, South Africa (2007)
12. *Coordinador Eléctrico*: *INFOTECNICA – Información de Instalaciones*. (Chilean ISO, Technical Information of Infrastucture), Accessed April 15, 2021 at https://infotecnica.coordinador.cl/instalaciones/unidades-generadoras
13. Dán, G., Sandberg, H.: Stealth attacks and protection schemes for state estimators in power systems. In: 2010 First IEEE International Conference on Smart Grid Communications, pp. 214–219. Gaithersburg, MD, USA (2010)
14. Dunning, I., Huchette, J., Lubin, M.: Jump: A modeling language for mathematical optimization. SIAM Review **59**(2), 295–320 (2017). DOI 10.1137/15M1020575
15. Eaton Corporation: Substation automation: fundamentals of substation automation. Accessed June 15, 2020 at https://www.eaton.com/us/en-us/products/utility-grid-solutions/grid-automation-system-solutions/fundamentals-of-substation-automation.html
16. Falahati, B., Kargarian, A., Fu, Y.: Impacts of information and communication failures on optimal power system operation. In: 2013 IEEE PES Innovative Smart Grid Technologies Conference (ISGT). Washington, DC, USA (2013)
17. Golshani, A., Sun, W., Zhou, Q., Zheng, Q.P., Hou, Y.: Incorporating wind energy in power system restoration planning. IEEE Transactions on Smart Grid **10**(1), 16–28 (2019). DOI 10.1109/TSG.2017.2729592
18. Gungor, V., Lambert, F.: A survey on communication networks for electric system automation. Computer Networks **50**(17), 877–897 (2006). DOI 10.1016/j.comnet.2006.01.005
19. Hong, T., Hofmann, A.: Data integrity attacks against outage management systems. IEEE Transactions on Engineering Management pp. 1–8 (2021). DOI 10.1109/TEM.2021.3055139
20. Igure, V.M., Laughter, S.A., Williams, R.D.: Security issues in scada networks. Computers and Security **25**(7), 498–506 (2006). DOI 10.1016/j.cose.2006.03.001
21. Kocuk, B., Dey, S.S., Sun, X.A.: Strong SOCP relaxations for the optimal power flow problem. Operations Research **64**(6), 1177–1196 (2016). DOI 10.1287/opre.2016.1489
22. Lai, K., Illindala, M., Subramaniam, K.: A tri-level optimization model to mitigate coordinated attacks on electric power systems in a cyber-physical environment. Applied Energy **235**, 204–218 (2019). DOI 10.1016/j.apenergy.2018.10.077
23. National Hurricane Center and Central Pacific Hurricane Center: Hurricane harvey advisory number 23 (2017). Accessed June 18, 2020 at https://www.nhc.noaa.gov/archive/2017/al09/al092017.public.023.shtml?
24. Nemhauser, G.L., Wolsey, L.A.: Integer and Combinatorial Optimization. John Wiley & Sons, Inc., Hoboken, NJ (1999)
25. Panteli, M., Kirschen, D.S.: Assessing the effect of failures in the information and communication infrastructure on power system reliability. In: 2011 IEEE/PES Power Systems Conference and Exposition. Phoenix, AZ (2011)
26. Parandehgheibi, M., Modiano, E., Hay, D.: Mitigating cascading failures in interdependent power grids and communication networks. In: 2014 IEEE International Conference on Smart Grid Communications, pp. 242–247. Venice, Italy (2014)

27. Patsakis, G., Rajan, D., Aravena, I., Oren, S.: Strong mixed-integer formulations for power system islanding and restoration. IEEE Transactions on Power Systems **34**(6), 4880–4888 (2019)
28. Rahnamay-Naeini, M., Hayat, M.M.: On the role of power-grid and communication-system interdependencies on cascading failures. In: 2013 IEEE Global Conference on Signal and Information Processing, pp. 527–530. Austin, TX, USA (2013)
29. Sridhar, S., Hahn, A., Govindarasu, M.: Cyber-physical system security for the electric power grid. Proceedings of the IEEE **100**(1), 210–224 (2012)
30. Stouffer, K., Pillitteri, V., Lightman, S., Abrams, M., Hahn, A.: NIST special publication 800-82, revision 2, guide to industrial control systems (ICS) security. Tech. rep., National Institute of Standards and Technology, U.S. Department of Commerce (2015). URL `http://dx.doi.org/10.6028/NIST.SP.800-82r2`
31. Sun, W., Liu, C., Zhang, L.: Optimal generator start-up strategy for bulk power system restoration. IEEE Transactions on Power Systems **26**(3), 1357–1366 (2011). DOI 10.1109/TPWRS.2010.2089646
32. Systems Operations Division: PJM manual 36: System restoration. Tech. rep., PJM (2021). URL `https://www.pjm.com/~/media/documents/manuals/m36.ashx`
33. Teixeira, A., Amin, S., Sandberg, H., Johansson, K.H., Sastry, S.S.: Cyber security analysis of state estimators in electric power systems. In: 49th IEEE Conference on Decision and Control, pp. 5991–5998. Atlanta, GA, USA (2010)
34. Ten, C.W., Liu, C.C., Manimaran, G.: Vulnerability assessment of cybersecurity for SCADA systems. IEEE Transactions on Power Systems **23**, 1836–1846 (2008). DOI 10.1109/TPWRS.2008.2002298
35. The National Academies of Sciences, Engineering, and Medicine: Enhancing the resilience of the nation's electricity system. Tech. rep., The National Academies Press, Washington, DC, USA (2017). URL `https://doi.org/10.17226/24836`
36. United States Geological Surgey: Flood Event Viewer - Harvey 2017. Accessed June 18, 2020 at `https://stn.wim.usgs.gov/fev/#HarveyAug2017`
37. Van Hentenryck, P., Coffrin, C.: Transmission system repair and restoration. Mathematical Programming **151**(1), 347–373 (2015). DOI 10.1007/s10107-015-0887-0. URL `https://doi.org/10.1007/s10107-015-0887-0`
38. Xie, Z., Manimaran, G., Vittal, V., Phadke, A.G., Centeno, V.: An information architecture for future power systems and its reliability analysis. IEEE Transactions on Power Systems **17**, 857–863 (2002)
39. Zhang, S., Vittal, V.: Design of wide-area power system damping controllers resilient to communication failures. IEEE Transaction on Power Systems **28**, 4292–4300 (2013)
40. Zhong, J., Zhang, F., Yang, S., Li, D.: Restoration of interdependent network against cascading overload failure. Physica A: Statistical Mechanics and its Applications **514**, 884–891 (2019). DOI 10.1016/j.physa.2018.09.130

A Nomenclature

Sets:

N	buses
N_t^-	buses that have not been energized by time t
G	the complete set of generators
G^{BS}	blackstart generators
$G(M)$	generators across a set of buses M
G_t^-	generators that have not been energized by time t
G_t^{CR-}	de-energized generators that have not begun cranking by time t
L	the complete set of transmission lines
$L(\delta M)$	the set of transmission lines with exactly one terminal within the bus set M
L_t^-	lines that have not been energized by time t
SC	series compensators
$SC(M)$	series compensators across a set of buses M
C	control centers
C_0	control centers for which communications equipment is operational from the start of the time horizon ($C_0 \subseteq C$)
C_t^-	damaged control centers for which communication repairs have not begun by time t

S	substations
S_0	substations for which communications equipment is operational from the start of the time horizon ($S_0 \subseteq S$)
$S(c)$	substations controlled by control center c
S_t^-	damaged substations for which communication repairs have not begun by time t
L^{comm}	communications channels
$I(\ell)$	terminals (buses) of branch ℓ
$I^{\text{comm}}(\ell)$	terminals (substations or control centers) of communications channel ℓ
$T = \{1, \ldots, \overline{T}\}$	time periods in the restoration horizon

Index Maps:

$n(g)$	bus of generator g
$s(n)$	substation of bus n
$c(n)$	control center controlling substation of bus n

Parameters:

CT_g	cranking time of generator g
τ_a	number of time periods required to repair communications equipment at substation or control center a
K	maximum number of transmission element energizations between snapshots
K^{comm}	number of technicians available to repair communications equipment
β_a	benefit of energizing component a
J_g	inertia constant of generator g
$\alpha, \Theta(\cdot)$	objective coefficient and benefit function for system inertia
γ	time-based discount rate
γ^{dist}	distance-based discount rate
$u_{a,0}, w_{a,0}$	initial status of component a, where $u_{a,t}$ and $w_{a,t}$ are as defined for variables below

Variables:

$u_{a,t}$	binary variable that is 1 if power system component a is energized at time t, 0 otherwise
$u_{g,t}^{\text{CR}}$	binary variable that is 1 if generator g is cranking at time t, 0 otherwise
$w_{a,t}$	binary variable that is 1 if control center, substation, or communications channel a is operational at time t, 0 otherwise
$w_{a,t}^{\text{rep}}$	binary variable that is 1 if repair begins on control center or substation $a \in \{C \backslash C_0\} \cup \{S \backslash S_0\}$ at time t, 0 otherwise (undefined for $a \in C_0 \cup S_0$)

Graph Definitions

$\mathscr{G}_t$	graph of the communications system in which connected components of operational communications elements at time t are grouped into super-nodes
$\mathscr{G}_{ct}$	subset of the graph $\mathscr{G}_t$ associated with control center c
$v_t(a)$	the node in graph $\mathscr{G}_t$ associated with element a
$MST(\mathscr{G}_{ct})$	minimum spanning tree of $\mathscr{G}_{ct}$, where edge weights are based on repair times
$N_t(v)$	the set of buses associated with node v of the graph $\mathscr{G}_t$ (accounting for super-nodes)
$\mathscr{V}_{ct}(v)$	the set of nodes for which node v is along the path to from the control center c in $MST(\mathscr{G}_{ct})$
$\delta_{v_1 v_2 ct}$	the (weighted) distance from node v_1 to v_2 in $MST(\mathscr{G}_{ct})$

B Formulation for optimal power system restoration

We represent the energization status of any component in the system using the binary variable $\mathbf{u}$, with appropriate subindexes, which takes the value 1 if the component is energized and 0 otherwise. Additionally, we use binary variables $\mathbf{u}^{\mathrm{CR}}$ to indicate whether generators are cranking or not.

$$u_{n,t}, u^{\mathrm{CR}}_{n,t} \in \{0,1\} \; \forall \, n \in N, t \in T \tag{16}$$

Energization requirements for generators are modeled as Constraints (17), where we use $(\cdot)^+$ to denote the positive part operator, which is implemented using its standard linear programming reformulation (omitted here for brevity).

$$u^{\mathrm{CR}}_{g,t} \leq u_{g,t} \quad \forall g \in G, t \in T \tag{17a}$$

$$\sum_{\tau=t-CT_g+1}^{t} (u_{g,\tau} - u_{g,\tau-1})^+ \leq u^{\mathrm{CR}}_{g,t} \quad \forall g \in G, t \in T \tag{17b}$$

$$u^{\mathrm{CR}}_{g,t} \leq u_{n(g),t} \quad \forall g \in G \setminus G^{BS}, t \in T \tag{17c}$$

$$u_{g,t} - u^{\mathrm{CR}}_{g,t} \leq u_{n(g),t} \quad \forall g \in G, t \in T \tag{17d}$$

We formulate the bus energization requirement as Constraints (18). These constraints are exponentially many in terms of $|N|$, however, they can be separated in polynomial time in a similar manner to Constraints (9) [27].

$$u_{n,t} \leq \sum_{g \in G(M)} (u_{g,t} - u^{\mathrm{CR}}_{g,t}) + \sum_{\ell \in L(\delta M)} u_{\ell,t} \; \forall \, M \subseteq N : SC(\delta M) = \emptyset, n \in M, t \in T \tag{18}$$

Restrictions on energization of branches are modeled as Constraints (19).

$$u_{\ell,t} \leq \sum_{n \in I(\ell)} u_{n,t-1} \quad \forall \ell \in L, t \in T \tag{19a}$$

$$u_{\ell,t} \leq u_{n,t} \quad \forall \ell \in L, n \in I(\ell), t \in T \tag{19b}$$

$$\sum_{\ell \in L} (u_{\ell,t} - u_{\ell,t-1})^+ \leq K \quad \forall t \in T \tag{19c}$$

In order for the restoration plan to be feasible, the energized elements in the power grid must, at least, admit a valid power flow solution at each snapshot $t \in T$. That is, there needs to exist voltage settings and power injections that satisfy the power flow equations, and thermal and security limits of the power grid. We formulate a relaxation of this requirement, namely

$$(u_t, u^{\mathrm{CR}}_t) \in \mathscr{P}^{SOCP} \quad \forall t \in T, \tag{20}$$

where $\mathscr{P}^{SOCP}$ is the set of system configurations that admit feasible solutions to the second-order cone relaxation to the optimal power flow problem as described in [21].

Finally, we use (21) as our objective function.

$$\max \; \sum_{t \in T} \left(\alpha \cdot \Xi \left(\sum_{g \in G} J_g \cdot \left(u_{g,t} - u^{\mathrm{CR}}_{g,t} \right) \right) + \sum_{\ell \in L} \beta_\ell u_{\ell,t} + \sum_{n \in N} \beta_n u_{n,t} \right) \tag{21}$$

Here the term in the first line uses system inertia as a surrogate for stability and the terms in the second line use the energization status of branches and buses as a surrogate for coverage. Ξ is a piecewise concave increasing function that cuts off contributions above normal-operation inertia to the objective function. Parameters $\alpha > 0$ and $\beta > 0$ are set following priorities for restoration of the system under consideration.

The OPSR problem corresponds to the mathematical program (16) – (21). The OPSR-C problem is a restriction of the OPSR problem and can be expressed as the mathematical program $\{(1) – (9), (11), (16) – (21)\}$; or, equivalently, $\{(1) – (11), (21)\}$, where $\mathscr{E}$ is defined as follows:

$$\begin{aligned} \mathscr{E} := \; \big\{ v \in \{0,1\}^{|N| \times |T|} \mid \exists (u, u^{\mathrm{CR}}) \in & \{0,1\}^{(|N|+|L|+|G|) \times |T|} \times \{0,1\}^{|G| \times |T|} : \\ & (17) – (20), u_{n,t} = v_{n,t} \; \forall n \in N, t \in T \big\} \end{aligned} \tag{22}$$